sustainability

Article

Stability of Unsaturated Soil Slope Considering Stratigraphic Uncertainty

Wei Cao [1,2,*], Zheng Wan [2] and Wenjing Li [3]

1 School of Transportation Science and Engineering, Beihang University, Beijing 100191, China
2 School of Architectural Engineering, North China Institute of Science and Technology, Langfang 065201, China; zhengw111@126.com
3 School of Architecture, Yanching Institute of Technology, Langfang 065201, China; liwenjing@yit.edu.cn
* Correspondence: by1713111@buaa.edu.cn; Tel.: +86-151-3267-1856

Abstract: Stratigraphic uncertainty is widely present in nature, but it has not been well considered in the stability analysis of unsaturated soil slopes in the past. In this study, the stability of the unsaturated soil slope is evaluated based on borehole data considering stratigraphic uncertainty. Firstly, an enhanced coupled Markov chain model is used to simulate stratigraphic uncertainty. Then, a finite element algorithm for automatically calculating the safety factor (*FS*) and the average groundwater table (*AGT*) of the unsaturated soil slope is developed. At last, a hypothetical slope located in the stratum from Perth, West Australia is analyzed using the proposed algorithm under different borehole schemes. The results show that with the increase in the borehole number, the statistics of *FS* and *AGT* will not monotonically increase or decrease. But the trend is that the mean values of *FS* and *AGT* gradually approach and eventually converge to the real values, and the standard deviations of *FS* and *AGT* decrease. There is a linear relationship between the standard deviation of *FS* (or *AGT*) and the average information entropy. The *FS* and *AGT* are negatively correlated considering stratigraphic uncertainty.

Keywords: stratigraphic uncertainty; unsaturated soil; slope stability; coupled Markov chain; groundwater table; finite element

check for updates

Citation: Cao, W.; Wan, Z.; Li, W. Stability of Unsaturated Soil Slope Considering Stratigraphic Uncertainty. *Sustainability* **2023**, *15*, 10717. https://doi.org/10.3390/su151310717

Academic Editor: Chaolin Zhang

Received: 5 June 2023
Revised: 5 July 2023
Accepted: 5 July 2023
Published: 7 July 2023

1. Introduction

Natural soils often exhibit various types of uncertainty due to material composition, depositional conditions, stress history, weathering, and other geological effects [1,2]. The uncertainty can be mainly divided into two categories: inherent variability of soil parameters and stratigraphic uncertainty [3,4]. The inherent variability of soil parameters is the difference in soil parameters at different spatial points within one nominally homogeneous layer. Many random field models, such as stationary and non-stationary random fields [5,6], isotropic and anisotropic random fields [7] and conditional and unconditional random fields [8], are usually used for characterizing the inherent variability of soil parameters. Stratigraphic uncertainty is specific to the heterogeneous layer and refers to the fact that different types of soil are usually staggered in the actual stratum. More and more attention has been paid to stratigraphic uncertainty, and several methods have been proposed to simulate stratigraphic uncertainty. Tang et al. [9] proposed a model to describe the stratum consisting of two soil types. Kohno et al. [10] introduced a Poisson process to simulate the distribution of rock types along the tunnel axis. These two models can be utilized to simulate the strata containing two types of soil. However, none of these approaches is sufficiently suitable for the strata containing more types of soil. Elfeki and Dekking [11,12] proposed the coupled Markov chain (CMC) model for simulating stratigraphic uncertainty based on borehole data. Li et al. [13] and Wang et al. [14,15] put forward a kind of Markov random field theory to simulate stratigraphic uncertainty, but in this method, the orientation of the strata should be known in advance. Wang et al. [16] and Cao et al. [17] believed that machine learning can solve many engineering problems [18,19], including simulating stratigraphic uncertainty. They used Bayesian identification approaches for underground soil stratum identification and soil classification based on cone penetration tests. Other models, such as the random field-based approach [20] and the multiple point statistics approach [21], have recently been presented to describe stratigraphic uncertainty. Among these models, the CMC model is widely used in stratigraphic modeling for its simplicity in theory and other advantages [22]. Based on the CMC model, some improvements have been made by researchers to enhance the abilities of stratigraphic uncertainty simulation [23–25]. For example, to apply the CMC model to small-scale geological engineering problems, Qi et al. [22,26] proposed a method to estimate the horizontal transition probability matrix (HTPM) by using borehole data. Li et al. [27] developed a direction-dependent CMC model to solve the problem of simulating the strata with different dip directions and prisms.

It has been recognized that uncertainty has a significant influence on the stability of geological structures such as slopes. However, in the stability analysis of unsaturated soil slope, the stratum was usually considered to be deterministic in the past [28–35]. Recently, increasing attention has been paid to the unsaturated slope stability analysis considering the spatial variability of soil properties [36–42]. For example, Srivastava et al. [43] treated the value of saturated hydraulic conductivity as a random variable distributed in the stratum and investigated the effect of the variability of the permeability properties on slope stability analysis. Jiang et al. [44] proposed a non-intrusive stochastic finite element method based on Latin hypercube sampling and applied it to the reliability analysis of unsaturated soil slopes considering the spatial variability of multiple soil parameters. Le et al. [45,46] studied the failure probability and the size of failure of an unsaturated soil slope under constant rainfall considering the spatial variability of porosity. The saturated permeability was considered to be related to the porosity. The results indicated that the mean value and the variability of the safety factor (*FS*) depended on the correlation length and the coefficient of variation of the porosity field. Ng et al. [47] investigated the influence of 3D rotational anisotropy of the permeability coefficient on the reliability of unsaturated soil slope under rainfall infiltration. An ABAQUS-Matlab-Python interface framework was adopted to perform random finite element analysis. Python script was applied to extract required results such as groundwater table and *FS*. The results showed that the rotational anisotropy of permeability coefficient has a significant influence on the groundwater table and *FS*. These studies have quantified the influence of inherent spatial variability of soil parameters on the unsaturated slope stability analysis. However, few studies have incorporated the effect of stratigraphic uncertainty on the stability of unsaturated soil slopes. Until now, the existing research on slope stability analysis considering stratigraphic uncertainty has been limited to dry or saturated slope. Rotaru et al. [48] investigated the slip surface and *FS* of slope with four different soil characteristics using the limit equilibrium method and the finite element method (FEM). He pointed out that for non-homogeneous slopes, the discontinuity of the soil parameters will lead to discontinuities of the stress field, and then lead to the difficulty to determine the critical slip surface and *FS*. Li et al. [49] first introduced stratigraphic uncertainty into the reliability analysis of slopes and investigated the influence of borehole schemes on the slope safety factor and failure probability. Liu et al. [50] studied the effect of the stratigraphic boundary uncertainty on the reliability analysis of slope in spatially variable soils and found that the traditional reliability analysis of slope with deterministic stratigraphic boundary conditions can overestimate the reliability of slope. Gong et al. [51] used the stochastic Markov random field-based approach to simulate stratigraphic uncertainty and studied the influence of stratigraphic uncertainty on a slope reinforced by a single row of stabilizing piles. Ghadrdan et al. [52] proposed a simplified method for probabilistic stratigraphic analysis within a finite element software to assess the influence of stratigraphic uncertainty on slope stability. Deng et al. [3,53] proposed a slope reliability analysis method considering both the inherent variability of soil parameters and stratigraphic uncertainty. The results showed that these two uncertainties have a non-negligible impact on the reliability of slopes.

This paper aims to study the influence of stratigraphic uncertainty on unsaturated soil slope stability. The enhanced CMC model with an analytical method for estimating HTPM is utilized to simulate stratigraphic uncertainty. The concept of information entropy is adopted to quantify the level of stratigraphic uncertainty. Then the simulated strata are mapped into the finite element method model of the unsaturated soil slope to analyze the stability of slopes. Based on the proposed numerical implementation strategies, a hypothetical unsaturated soil slope located in the stratum in Australia consisting of three soil types is taken as an example to study the influence of stratigraphic uncertainty on slope stability. Different borehole layout schemes are designed to study their effect on the statistics (including mean value and standard deviation) of safety factor and groundwater table.

2. Methodology

2.1. Enhanced CMC Model for Simulating Stratigraphic Uncertainty

Markov property means that the future state only depends on the current state rather than previous states and it is widely present in strata. Elfeki and Dekking [11,12] coupled two Markov chains in the horizontal and vertical directions and proposed the CMC model. The CMC model is an effective approach for simulating stratigraphic uncertainty in practical engineering [49,54]. But in geotechnical engineering problems, the boreholes are usually sparse due to budget restrictions. Therefore, the horizontal transition probability matrix (HTPM) of the CMC model is difficult to determine. Two improvements have been made to enhance the traditional CMC method. Firstly, an analytical method for estimating HTPM based on the maximum likelihood estimation method is proposed. Secondly, the simulation sequence is determined by the overall tendency of strata [55], not always from left to right. To solve this problem, an analytical method for estimating HTPM is proposed and then used to enhance the traditional CMC model. In the estimation of HTPM, the only parameter to be determined is K (Walther's constant). The K value corresponding to the maximum value of the likelihood L of the observed scenario (see Figure 1) is taken as the estimated K. After the K value is estimated, the HTPM can be calculated based on Walther's law. Note that the K value should be calculated both from left to right and from right to left (denoted as K_{LR} and K_{RL}, respectively), and the larger one of K_{LR} and K_{RL} is taken as the estimated K. As shown in Figure 1, when estimating the K value from left to right, the likelihood of the observed scenario can be expressed as [20]:

$$L = \prod_{i=2}^{N-1} \left(\frac{p^{h(C_i-C_{i-1})}_{S_{C_{i-1},1},S_{C_i,1}} p^{h(N_x-C_i)}_{S_{C_i,1},S_{N_x,1}}}{p^{h(N_x-C_{i-1})}_{S_{C_{i-1},1},S_{N_x,1}}} \frac{p^{h(C_i-C_{i-1})}_{S_{C_{i-1},2},S_{C_i,2}} p^{h(N_x-C_i)}_{S_{C_i,2},S_{N_x,2}} p^{v}_{S_{C_i,1},S_{C_i,2}}}{\sum_{f=1}^{n} p^{h(C_i-C_{i-1})}_{S_{C_{i-1},2},f} p^{h(N_x-C_i)}_{f,S_{N_x,2}} p^{v}_{S_{C_i,1},f}} \cdots \frac{p^{h(C_i-C_{i-1})}_{S_{C_{i-1},N_z},S_{C_i,N_z}} p^{h(N_x-C_i)}_{S_{C_i,N_z},S_{N_x,N_z}} p^{v(N_z-1)}_{S_{C_i,1},S_{C_i,N_z}}}{\sum_{f=1}^{n} p^{h(C_i-C_{i-1})}_{S_{C_{i-1},N_z},f} p^{h(N_x-C_i)}_{f,S_{N_x,N_z}} p^{v(N_z-1)}_{S_{C_i,1},f}} \right), \quad (1)$$

where p_{ij}^h and p_{ij}^v are the elements of HTPM and vertical transition probability matrix (VTPM), respectively. $s_{i,j}$ represents the soil state at cell (i, j). C_i represents the column where borehole i is located. N_x and N_z stand for the numbers of soil cells in the horizontal and vertical directions, respectively.

Once the HTPM is estimated, the enhanced CMC model can be utilized to simulate the strata following a specific sequence. The generating sequence is also determined by the relationship of K_{LR} and K_{RL}. If $K_{\mathrm{LR}} \geq K_{\mathrm{RL}}$, the generating sequence is from left to right. If $K_{\mathrm{LR}} < K_{\mathrm{RL}}$, the generating sequence is from right to left. As shown in Figure 2, when the generating sequence is from left to right, the probability of state S_k at cell (t, j) can be calculated by

$$P_{lm,k|q} = \Pr\left(Z_{t,j} = S_k \mid Z_{t-1,j} = S_l, Z_{t,j-1} = S_m, Z_{C_{i+1},j} = S_q\right) = \frac{p^h_{lk} p^{h(C_{i+1}-t)}_{kq} p^v_{mk}}{\sum_{f=1}^{n} p^h_{lf} p^{h(C_{i+1}-t)}_{fq} p^v_{mf}}, k = 1, \cdots, n, \quad (2)$$

where S_l, S_m and S_q are the states of the cells $(t-1, j)$, $(t, j-1)$ and (C_{i+1}, j), respectively. $p_{kq}^{h(C_{i+1}-t)}$ is the $(C_{i+1}-t)$-step horizontal transition probability from S_k to S_q, and p_{mk}^{v} is the one-step vertical transition probability from S_q to S_k.

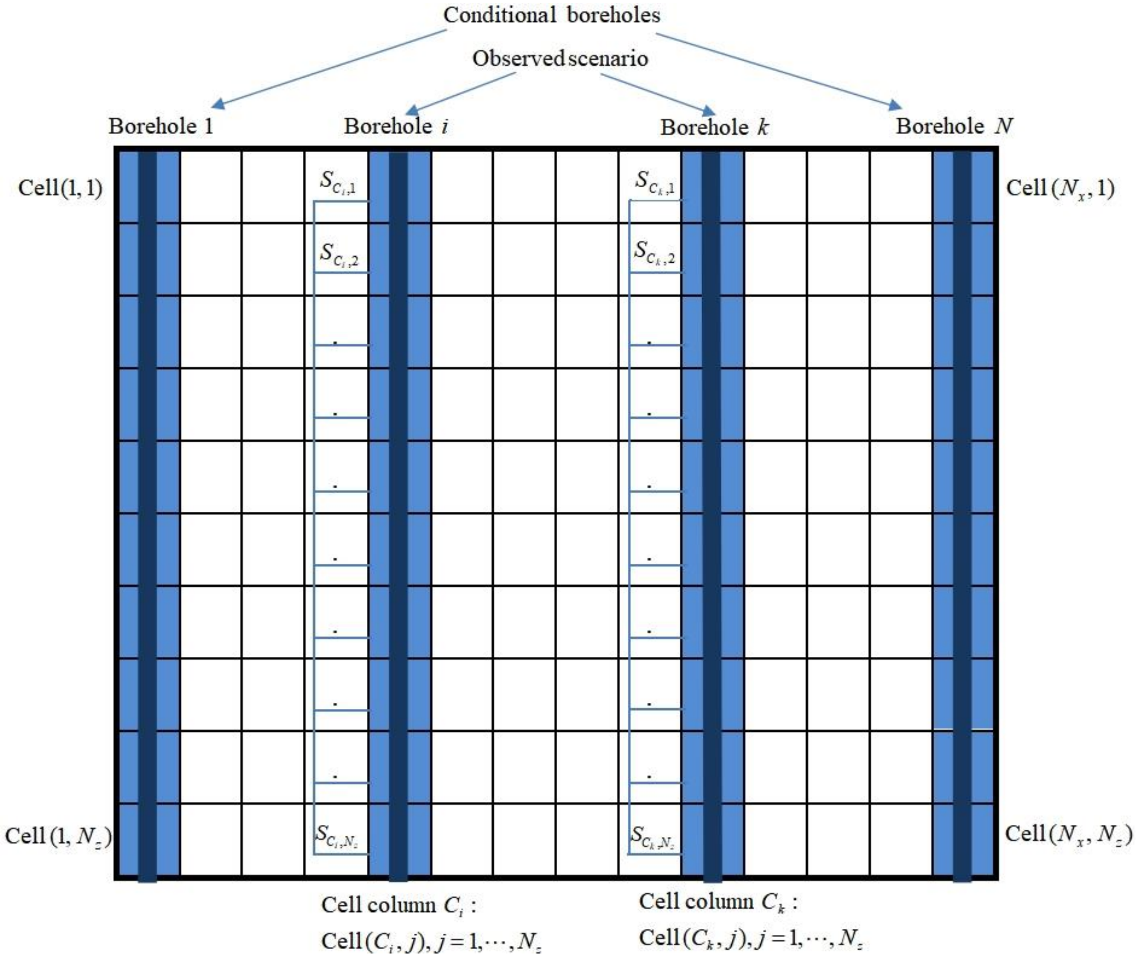

Figure 1. Conditional boreholes and observed scenario.

Two information entropy indexes are introduced to quantify the uncertainty of strata. One information entropy index is H_{ij}, which represents the uncertainty for soil cell (i, j) of the stratum, and it is defined as:

$$H_{ij} = -\sum_{k=1}^{m} p_{ij}^{k} \ln\left(p_{ij}^{k}\right) (i = 1, 2, \cdots, N_x; j = 1, 2, \cdots, N_z), \tag{3}$$

where m is the number of the soil types in the stratum, p_{ij}^{k} is the probability of soil type k occurring at soil cell (i, j). p_{ij}^{k} can be obtained by the frequency statistics from the simulated strata. The other information entropy index is called average information entropy (AVH), which is defined as the average value of H_{ij} of all the stratum soil cells:

$$AVH = \frac{1}{N_x N_z} \sum_{i=1}^{N_x} \sum_{j=1}^{N_z} H_{ij}. \tag{4}$$

The greater H_{ij} and AVH indicate the higher level of stratigraphic uncertainty at cell (i, j) and the whole stratum, respectively.

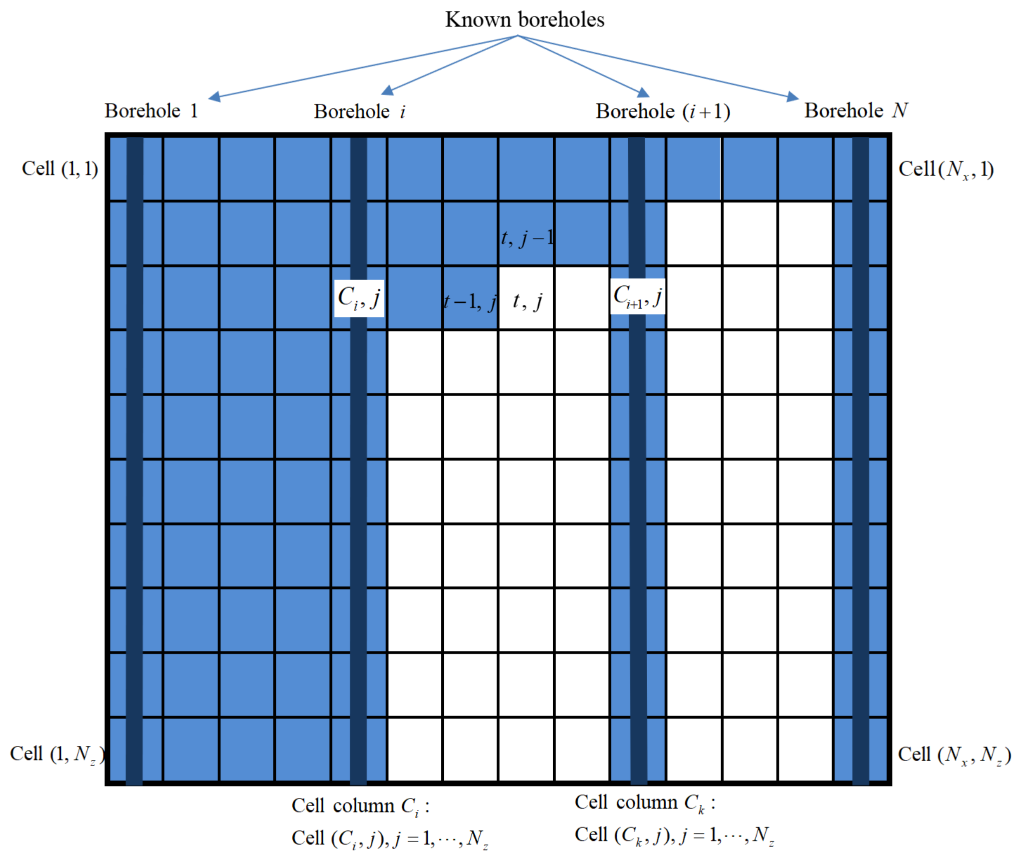

Figure 2. Generating the strata using the enhanced CMC model.

2.2. Mapping the Simulated Strata into the FEM Model of Slope

To consider the uncertainty of strata when analyzing the stability of unsaturated soil slope, the simulated strata should be mapped into the FEM model of slope. An initial FEM model with a homogeneous material needs to be established and the mesh should be the same with the simulated strata. Then we need to set up all the soil materials revealed in the boreholes and map the soil type distribution of the simulated strata into the FEM model of slope, which can be performed through the following three steps (see Figure 3): (i) Read the simulated strata information and store it in the matrix $Z(1{:}N_x,\ 1{:}N_z)$. For example, if $Z(i,j)$ = 'A' ($i = 1, \cdots, N_x, j = 1, \cdots, N_z$), the soil type of cell (i,j) is set to be type A. (ii) Calculate the coordinates of the center point of the meshed elements. (iii) Assign the soil material to all the elements according to the center point coordinates of the elements. If the coordinates of the center point of element η are $\left(x_c^{(\eta)}, z_c^{(\eta)}\right)$, the soil type $Z\left(\left\langle \frac{x_c^{(\eta)}}{\Delta x} \right\rangle, N_z + 1 - \left\langle \frac{z_c^{(\eta)}}{\Delta z} \right\rangle\right)$ ($\langle\theta\rangle$ denotes the minimum integer greater than θ, Δx and Δz are the horizontal and vertical length of the element, respectively) will be assigned to this element. After repeating these three steps until the entire simulated strata are mapped into the FEM model of slope, the FEM analysis can be performed on the slope features simulated strata. Note that the material type of element η is related to the coordinates of the element center point $\left(x_c^{(\eta)}, z_c^{(\eta)}\right)$; therefore, all the material parameters including γ (unit weight), E (Elastic modulus), ν (Poisson's ratio), c (effective cohesion), φ (effective friction angle), k (fully saturated hydraulic conductivity) and parameters for water retention model (i.e., the van Genuchten model). a and n are changed with the coordinates of the element center point $\left(x_c^{(\eta)}, z_c^{(\eta)}\right)$. If there are three soil types A (clay), B (sand) and C (silt), the material parameter vector $\boldsymbol{\Omega}^{(\eta)} = \left(\gamma^{(\eta)}, E^{(\eta)}, \nu^{(\eta)}, c^{(\eta)}, \varphi^{(\eta)}, k^{(\eta)}, a^{(\eta)}, n^{(\eta)}\right)$ of element η can be determined by the equation below:

$$\boldsymbol{\Omega}^{(\eta)} = \begin{cases} \boldsymbol{\Omega}_{\mathrm{A}} = (E_{\mathrm{A}}, \nu_{\mathrm{A}}, c_{\mathrm{A}}, \varphi_{\mathrm{A}}, k_{\mathrm{A}}, a_{\mathrm{A}}, n_{\mathrm{A}}), \left(Z\left(\left\langle \frac{x_c^{(\eta)}}{\Delta x} \right\rangle, N_z + 1 - \left\langle \frac{z_c^{(\eta)}}{\Delta z} \right\rangle\right) = \mathrm{A}\right) \\ \boldsymbol{\Omega}_{\mathrm{B}} = (E_{\mathrm{B}}, \nu_{\mathrm{B}}, c_{\mathrm{B}}, \varphi_{\mathrm{B}}, k_{\mathrm{B}}, a_{\mathrm{B}}, n_{\mathrm{B}}), Z\left(\left\langle \frac{x_c^{(\eta)}}{\Delta x} \right\rangle, N_z + 1 - \left\langle \frac{z_c^{(\eta)}}{\Delta z} \right\rangle\right) = \mathrm{B}) \\ \boldsymbol{\Omega}_{\mathrm{C}} = (E_{\mathrm{C}}, \nu_{\mathrm{C}}, c_{\mathrm{C}}, \varphi_{\mathrm{C}}, k_{\mathrm{C}}, a_{\mathrm{C}}, n_{\mathrm{C}}), Z\left(\left\langle \frac{x_c^{(\eta)}}{\Delta x} \right\rangle, N_z + 1 - \left\langle \frac{z_c^{(\eta)}}{\Delta z} \right\rangle\right) = \mathrm{C}) \end{cases}. \quad (5)$$

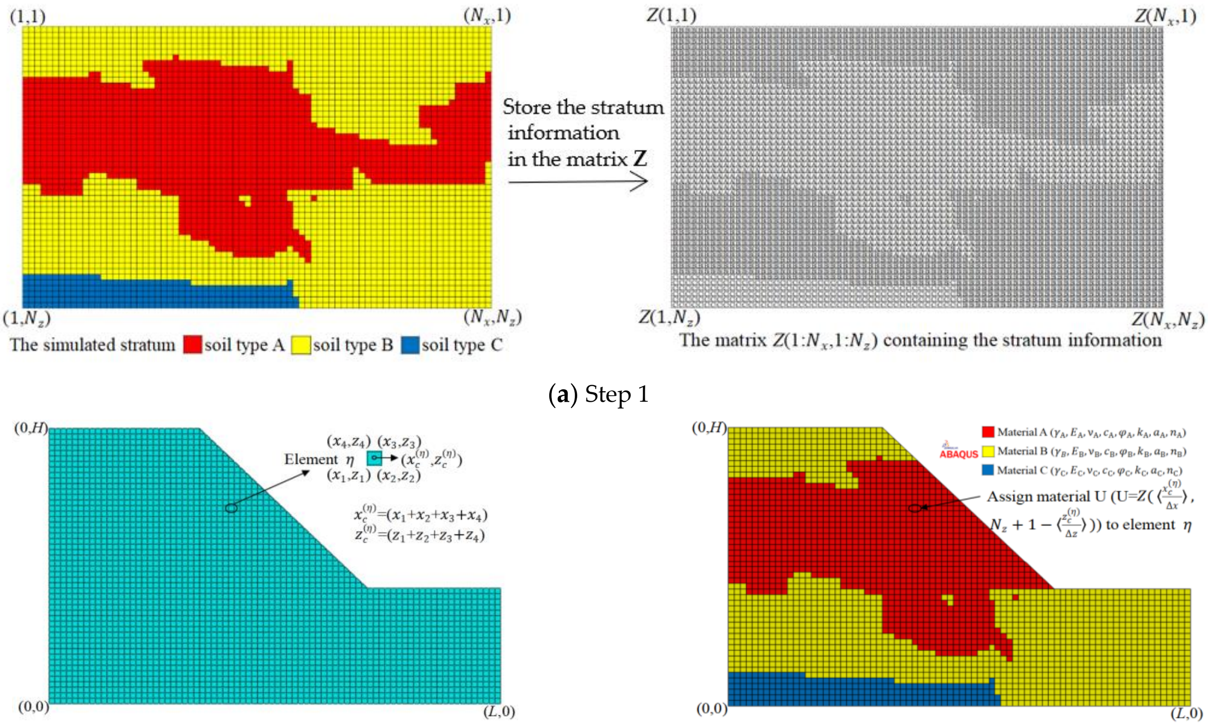

(**a**) Step 1

(**b**) Step 2 (**c**) Step 3

Figure 3. Steps of mapping the simulated strata into the FEM model of slope.

Therefore, the uncertainty of strata is considered in the stability analysis of unsaturated soil slope.

2.3. Coupled Pore Fluid Flow and Stress Analysis

The coupled global equations for unsaturated soil FEM analysis including the mechanical equilibrium equation and seepage equilibrium equation are shown below:

$$\mathbf{K}'\dot{\mathbf{U}} - \mathbf{L}\dot{\mathbf{U}}_{\mathrm{w}} = \dot{\mathbf{F}}^{\mathrm{ext}}, \quad (6)$$

$$\mathbf{L}'\dot{\mathbf{U}} + \mathbf{S}\dot{\mathbf{U}}_{\mathrm{w}} + \mathbf{H}\mathbf{U}_{\mathrm{w}} = \dot{\mathbf{Q}}^{\mathrm{ext}}, \quad (7)$$

where $\mathbf{U}$ and $\dot{\mathbf{U}}_{\mathbf{w}}$ are the vectors of nodal displacement and pore pressure, respectively. $\mathbf{L}$ and $\mathbf{L}'$ are coupling matrices, and $\mathbf{S}$ and $\mathbf{H}$ are seepage matrices. $\dot{\mathbf{F}}^{\mathbf{ext}}$ and $\dot{\mathbf{Q}}^{\mathbf{ext}}$ are the vectors of global external force rate and fluid supply, respectively. $\mathbf{K}'$ is the global stiffness matrix, and it has the following relationship with the element stiffness matrix:

$$\mathbf{K}' = \sum\nolimits_{\mathrm{elem.}} \int_{V_{\mathrm{elem.}}} \mathbf{B}_{\mathrm{u}}^{\mathrm{T}} \mathbf{D}'^{(\eta)} \mathbf{B}_{\mathrm{u}} \mathrm{d}V, \quad (8)$$

where $\mathbf{B}_\mathrm{u}$ is the strain-displacement shape function matrix, and $\mathbf{D}'^{(\eta)}$ is the stiffness matrix of element η.

Bishop's effective stress is adopted to describe the mechanical behavior of unsaturated soil. For element η, its formula is

$$\boldsymbol{\sigma}'^{(\eta)} = \boldsymbol{\sigma}^{(\eta)} + \left(\chi^{(\eta)} u_w^{(\eta)} + \left(1 - \chi^{(\eta)}\right) u_a^{(\eta)}\right)\mathbf{I}, \tag{9}$$

where $\boldsymbol{\sigma}'^{(\eta)}$ is the effective stress, $\boldsymbol{\sigma}'^{(\eta)}$ is the total stress and $u_w^{(\eta)}$ and $u_a^{(\eta)}$ are the pressure of liquid and gas, respectively. $\chi^{(\eta)}$ is an effective stress factor that depends on saturation. $\mathbf{I}$ is the identity matrix. Assuming that the air pressure $u_a^{(\eta)}$ is equal to zero and $\chi^{(\eta)}$ is taken as the degree of saturation $S_r^{(\eta)}$ for simplicity, Bishop's effective stress is defined as

$$\boldsymbol{\sigma}'^{(\eta)} = \boldsymbol{\sigma}^{(\eta)} + S_r^{(\eta)} u_w^{(\eta)}\mathbf{I}. \tag{10}$$

There is a relationship between saturation and matric suction $s^{(\eta)}$ ($s^{(\eta)} = -u_w^{(\eta)}$), which is characterized by the soil–water characteristic curve (SWCC). Herein the van Genuchten model is utilized to describe the SWCC curve,

$$S_r^{(\eta)} = \left[\frac{1}{1 + \left(s^{(\eta)}/a^{(\eta)}\right)^{n^{(\eta)}}}\right]^{(1-1/n^{(\eta)})}, \tag{11}$$

where $a^{(\eta)}$ and $n^{(\eta)}$ are the parameters of van Genuchten model and $a^{(\eta)}$ is usually called the air entry value. The values of $a^{(\eta)}$ and $n^{(\eta)}$ also change with the coordinates of the element center point. For the mechanical behavior, the stress–strain relationship is influenced by the matric suction. Therefore, the effective stress is used to describe mechanical behavior of the unsaturated soil. For element η, the formula of the elastic stress–strain is

$$\mathrm{d}\boldsymbol{\sigma}'^{(\eta)} = \mathbf{D}'^{(\eta)}\mathrm{d}\varepsilon^{(\eta)}. \tag{12}$$

The Mohr–Coulomb criterion is used to describe the shear strength of soil. The formula is

$$\frac{1}{2}\left(\sigma_1'^{(\eta)} - \sigma_3'^{(\eta)}\right) - \frac{1}{2}\left(\sigma_1'^{(\eta)} + \sigma_3'^{(\eta)}\right)\sin\varphi^{(\eta)} - c^{(\eta)}\cos\varphi^{(\eta)} = 0. \tag{13}$$

The values of $c^{(\eta)}$ and $\varphi^{(\eta)}$ are also related to the coordinates of the center point of meshed elements.

Darcy's law is used to describe the seepage law of liquid. The seepage matrix $\mathbf{H}$ is calculated by the equation below:

$$\mathbf{H} = -\sum\nolimits_{\mathrm{elem.}} \int_{V^{\mathrm{elem.}}} \mathbf{B}_\mathrm{w}^\mathrm{T} \frac{\overline{\mathbf{k}}^{(\eta)}}{\gamma_w} \mathbf{B}_\mathrm{w}\mathrm{d}V, \tag{14}$$

where $\mathbf{B}_\mathrm{w} = \nabla\mathbf{N}_\mathrm{w}$ ($\mathbf{N}_\mathrm{w}$ is the pore pressure shape function matrix), γ_w is the unit weight of pore fluid and $\overline{\mathbf{k}}^{(\eta)}$ is the matrix of unsaturated hydraulic conductivity for element η. The matrix of unsaturated hydraulic conductivity $\overline{\mathbf{k}}^{(\eta)}$ is calculated using the equations below:

$$\overline{\mathbf{k}}^{(\eta)} = k_s{}^{(\eta)}\mathbf{k}^{(\eta)}, \tag{15}$$

$$\mathbf{k}^{(\eta)} = \begin{bmatrix} k^{(\eta)} & 0 & 0 \\ 0 & k^{(\eta)} & 0 \\ 0 & 0 & k^{(\eta)} \end{bmatrix} = k^{(\eta)}\mathbf{I}, \tag{16}$$

where $k^{(\eta)}$ is fully saturated hydraulic conductivity and ${k_s}^{(\eta)}$ is a parameter that depends on the degree of saturation. Generally speaking, with the degree of saturation increases, the unsaturated hydraulic conductivity decreases. To describe this relationship, ${k_s}^{(\eta)} = \left(S_r^{(\eta)}\right)^3$ is adopted in this paper. In the homogeneous soil slope, the values of $k^{(\eta)}$ are unchanged for all the elements ($k^{(\eta)} = k_0$). While when the uncertainty of the strata is considered, the values of $k^{(\eta)}$ are related to the coordinates of the center point of meshed elements. Therefore, the seepage matrix $\mathbf{H}$ can be expressed as

$$\mathbf{H} = -\sum\nolimits_{\text{elem.}} \int_{V^{\text{elem.}}} \mathbf{B}_{\text{w}}^{\text{T}} \frac{k^{(\eta)} {k_s}^{(\eta)} \mathbf{I}}{\gamma_w} \mathbf{B}_{\text{w}} \text{d}V, \tag{17}$$

where the value of $k^{(\eta)}$ is determined by Equation (5).

2.4. Algorithm Development for Automatically Calculating the Safety Factor of Unsaturated Soil Slope

The stability analysis of slopes includes the limit equilibrium method, the finite element method, etc. [48]. The finite element method can consider the heterogeneity of soil and the nonlinearity of materials, and it does not need to assume the position of the sliding surface in advance. So, the finite element method is increasingly widely used in the slope stability analysis. In order to consider the uncertainty factors in slope stability analysis, many researchers [5,49,50] combined Monte Carlo simulation with finite element method to propose a stochastic finite element method for slope stability analysis. In this paper, an algorithm based on the stochastic finite element method for automatically calculating the safety factor of the unsaturated soil slope considering the uncertainty of strata is developed based on ABAQUS and built-in Python language. In the analysis program, ABAQUS software (version 6.14) is mainly used to calculate the safety factor of slope based on the strength reduction method and obtain the groundwater table. Python scripts are primarily utilized for the strata simulation, mapping the strata to FEM model, driving ABAQUS software for slope stability analysis, calculation results extraction, Monte Carlo simulation, statistical analysis, etc. There exists a stress field in the initial state of unsaturated soil slope under the action of gravity. Therefore, it is necessary to establish the initial stress field before the slope stability analysis. In the proposed analysis program, the initial stress field is obtained by analyzing the initial FEM model of slope with mapped strata using the "Soil (Steady State)" analyze step in ABAQUS. Then the initial stress field is incorporated into the FEM model of slope by editing the input file. The edited FEM model is further used to calculate the safety factor of slope using the strength reduction method. Similar to Liu et al. [50], the flow of the proposed program for analyzing the stability of unsaturated soil slope considering stratigraphic uncertainty is summarized in Figure 4. The whole procedure of the proposed program mainly includes ten steps. The details of each step are as follows:

(1) Collect the necessary data for slope stability modeling including the borehole data of the stratum, the parameters of various types of soil, the slope geometric parameters, the boundary conditions of slope and other information contained in the site.
(2) Discretize the stratigraphic profile into cells of appropriate size. Estimate the VTPM and HTPM based on the borehole data. Determine the simulation sequence according to the estimated values of K_{LR} and K_{RL}, and then use the enhanced CMC model introduced in Section 2.1 to generate the stratum.
(3) Establish the initial FEM model of slope in ABAQUS software based on the information collected in Step 1 including the geometry and the boundary conditions of slope.
(4) Map the simulated stratum into the FEM model of slope through python script and generate the input file named "Slope.inp".
(5) Calculate the initial stress field under the action of gravity by submitting the input file "Slope.inp" to analysis in ABAQUS. The initial stress field is saved in the "Slope.odb" file.

(6) Incorporate the initial stress field into the FEM model of slope and modify the finite element model by editing the "Slope.inp" file. The input file of the modified model is named "Slope-New.inp".
(7) Submit the "Slope-New.inp" file to the ABAQUS solver through python script. The safety factor of slope is calculated using the strength reduction method, and the results are stored in the file named "Slope-New.odb".
(8) Extract the calculation results such as safety factor and groundwater table of slope from the "Slope-New.odb" file using python script.
(9) Perform Monte Carlo simulation. Repeat steps 1–7 until the required N times are reached.
(10) Conduct statistical analysis based on the results containing the slope safety factor and the groundwater table.

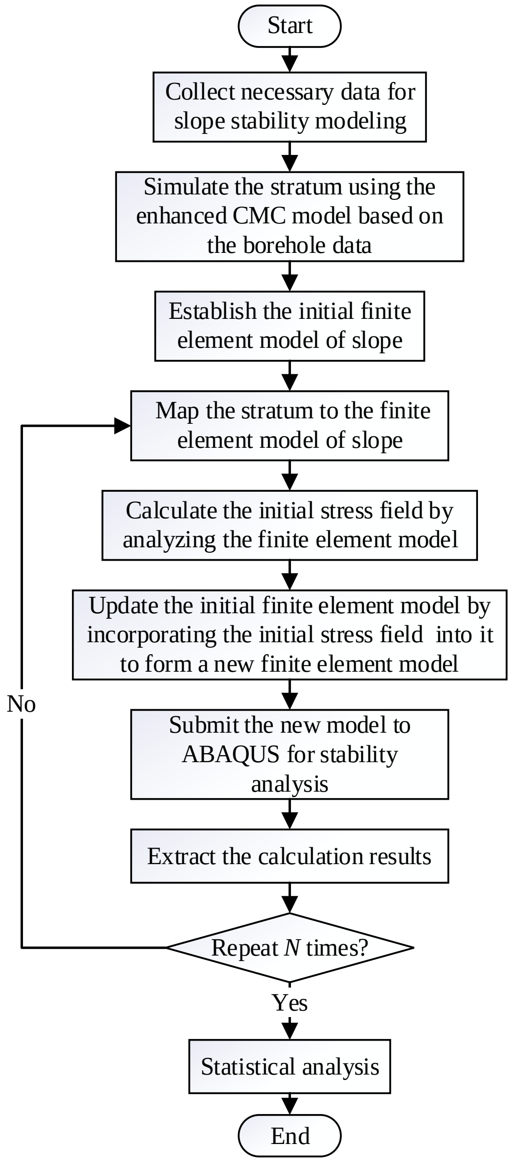

Figure 4. Flow chart of the proposed program.

3. Case Study

The proposed program is utilized in this section to evaluate the stability of an unsaturated soil slope under steady-state seepage flow considering stratigraphic uncertainty. The influence of borehole schemes on the slope stability evaluation and the groundwater table is investigated.

3.1. Borehole Data

The borehole data used in this paper are from Perth, West Australia collected by Li et al. [49]. This stratum contains a variety of soil types and shows obvious stratigraphic uncertainty. As shown in Figure 5a, to obtain the profile of the stratum, all the boreholes are projected in a straight line. Figure 5b shows the stratigraphic profile revealed by the six known boreholes. The stratigraphic profile is 70.2 m long and about 30.0 m deep. The soil layer within the boreholes can be classified into three types: clay, sand and silt.

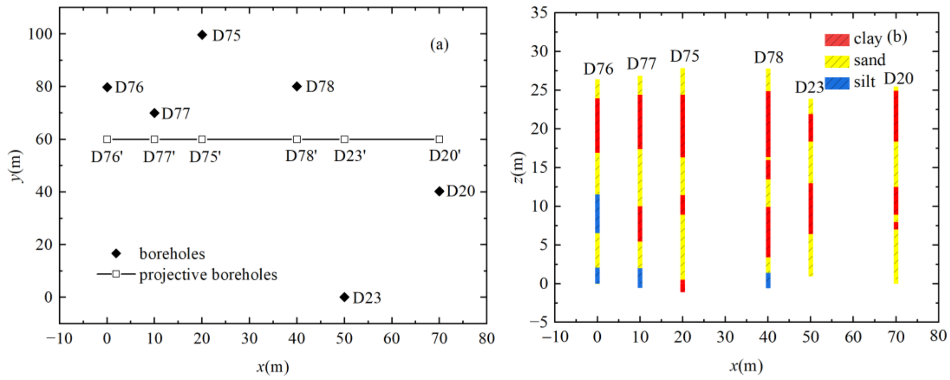

Figure 5. Borehole locations and distribution of soil types in the boreholes (after Li et al. [49]). (**a**) Relative location of the boreholes; (**b**) Distribution of soil types in the boreholes.

3.2. Simulation and Evaluation of Stratigraphic Uncertainty for Different Borehole Schemes

According to the minimum thickness of the geological unit in the boreholes and considering the calculation efficiency, the cell size 0.9 × 0.3 m^2 is used to divide the stratigraphic profile in this paper. After the first-order Markovian property of the stratum is confirmed by Li et al. [49] using the method of hypothesis test, the enhanced CMC model can be used for stratigraphic uncertainty simulation.

3.2.1. The "Real" Stratum

To test the difference between predicted and real results of the slope safety factor, the enhanced CMC model is used to generate a "real" stratum (see Figure 6). Due to the limited number of actual boreholes and the large spacing, to study the relationship between slope stability and borehole schemes, five virtual boreholes are selected in the "real" stratum. As shown in Figure 6, the eleven boreholes are re-labeled B1, B2, . . . , B11 from left to right for brevity. Assuming that there is a slope excavated in this stratum, and the geometry of the slope is also shown in Figure 6.

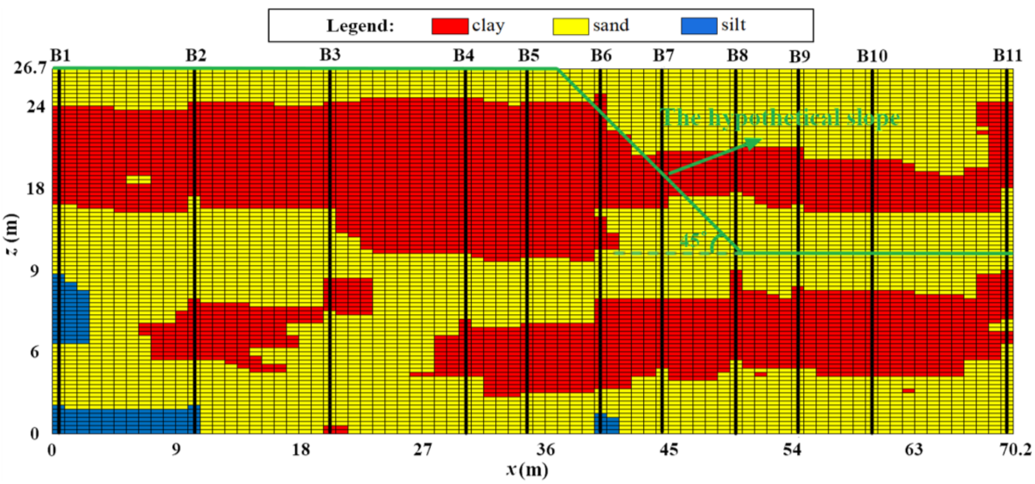

Figure 6. "Real" stratum and hypothetical slope.

3.2.2. Borehole Schemes

To investigate the influence of borehole schemes on the stability of the slope and the groundwater table, seventeen borehole schemes (see Table 1) are adopted to reflect the effect of both borehole number and location. In the borehole schemes, the number of boreholes ranges from 3 to 11. To study the overall trend of *FS* and groundwater table changing with the number of boreholes, 2–3 schemes are selected for the same number of boreholes, except for individual cases. Using the estimation method introduced in Section 2.1, the VTPM and HTPM for each borehole scheme can be estimated based on the known boreholes. For all the borehole schemes, the value of K_{LR} is always greater than or equal to K_{RL}. Thus, K_{LR} is taken as the estimated K value and the simulation sequence is from left to right. After estimating the VTPM, K and HTPM, the enhanced CMC model can be used to simulate the stratum of a specific borehole scheme.

Table 1. Different borehole schemes considered in the study.

Borehole Scheme	Number of Boreholes	B1	B2	B3	B4	B5	B6	B7	B8	B9	B10	B11
Scheme 1	3	√					√					√
Scheme 2	4	√		√			√					√
Scheme 3	4	√					√		√			√
Scheme 4	5	√		√			√		√			√
Scheme 5	5	√	√				√		√			√
Scheme 6	5	√	√	√			√					√
Scheme 7	6	√	√	√			√		√			√
Scheme 8	7	√	√	√	√		√		√			√
Scheme 9	7	√	√	√			√		√		√	√
Scheme 10	8	√	√	√	√		√		√		√	√
Scheme 11	9	√	√	√	√	√	√		√		√	√
Scheme 12	9	√	√	√	√		√	√	√		√	√
Scheme 13	9	√	√	√	√		√		√	√	√	√
Scheme 14	10	√	√	√	√		√	√	√	√	√	√
Scheme 15	10	√	√	√	√	√	√		√	√	√	√
Scheme 16	10	√	√	√	√	√	√	√	√		√	√
Scheme 17	11	√	√	√	√	√	√	√	√	√	√	√

Note: The symbol "√" indicates that the borehole is known.

3.2.3. Stratigraphic Uncertainty for Different Borehole Schemes

Due to different known boreholes, different borehole schemes show different levels of stratigraphic uncertainty. Two information entropy indexes introduced in Section 2.1 are used to evaluate the level of stratigraphic uncertainty of different borehole schemes. Take the number of simulations as 1000 and calculate the information entropy H_{ij} for every soil cell of the stratum by using Equation (3). Then the information entropy maps can be drawn to analyze stratigraphic uncertainty at different locations. Figure 7 shows the information entropy maps of Schemes 1–7. The information entropy map is affected by the borehole boundary conditions, the transition probability matrix (VTPM and HTPM), the borehole spacing and other factors. Generally speaking, the smaller the spacing between boreholes, the smaller the information entropy H_{ij} of the soil cell. But the information entropy of soil cells is also affected by borehole boundary conditions. The emergence of new soil types at the same height will increase the local information entropy.

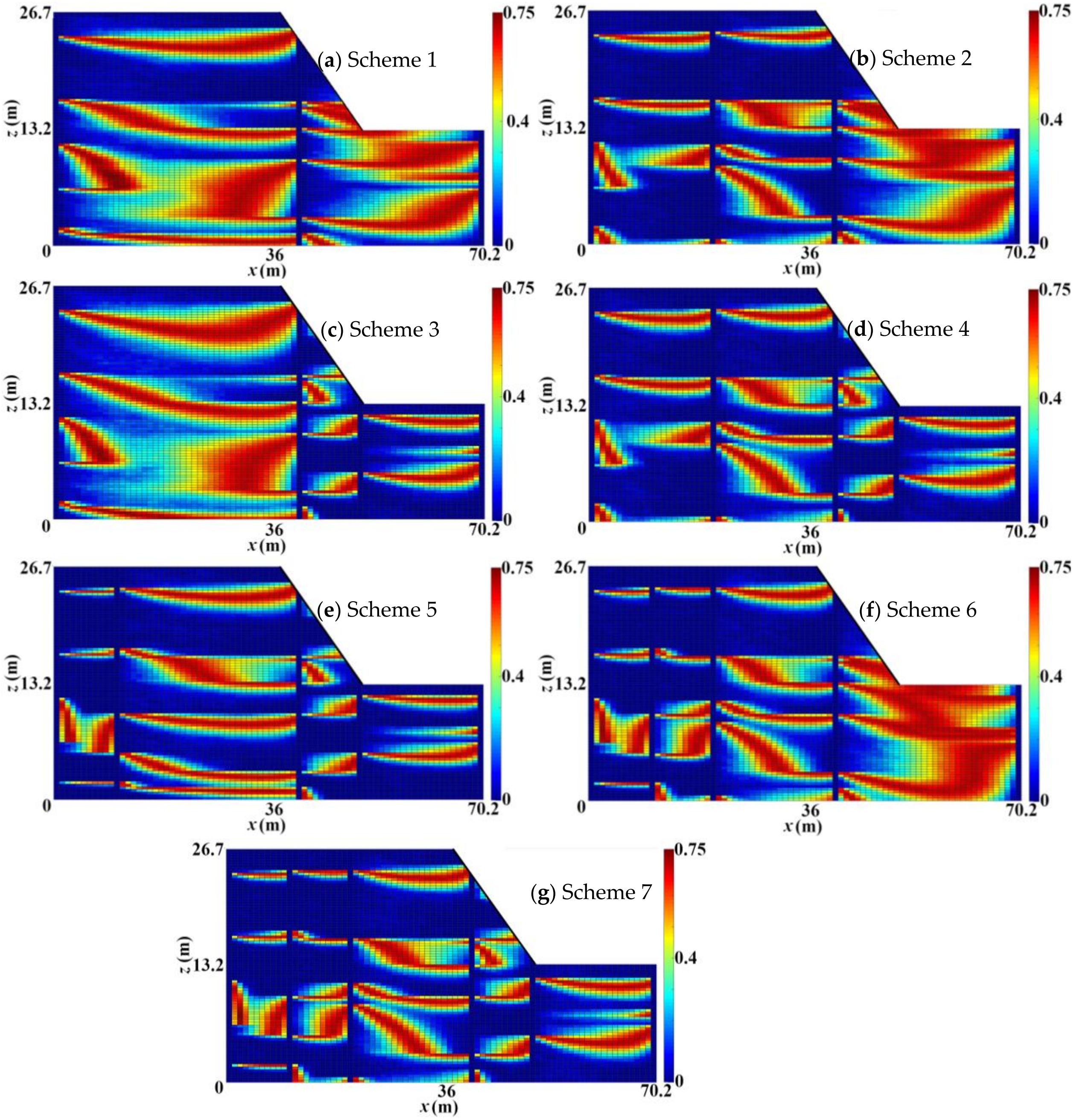

Figure 7. Information entropy maps for various borehole schemes.

The average information entropy AVH of the whole stratum, which is calculated by using Equation (4), is affected by the number of simulations. As shown in Figure 8, it can be seen that for all borehole schemes, the AVH remains stable when the number of simulations is more than 200. Therefore, 400 simulations are performed using the enhanced CMC model in this paper and the AVHs are calculated based on these simulated strata. The stable AVHs for different borehole schemes are different, which represent the different degrees of stratigraphic uncertainty. The AVHs for Scheme 1 and Scheme 17 are 0.302 and 0.118, respectively, which means that the simulated strata for Scheme 1 have higher uncertainty. Figure 9 shows the variations of AVH with the number of boreholes. As the number of boreholes increases, the AVH tends to decrease, but not monotonically.

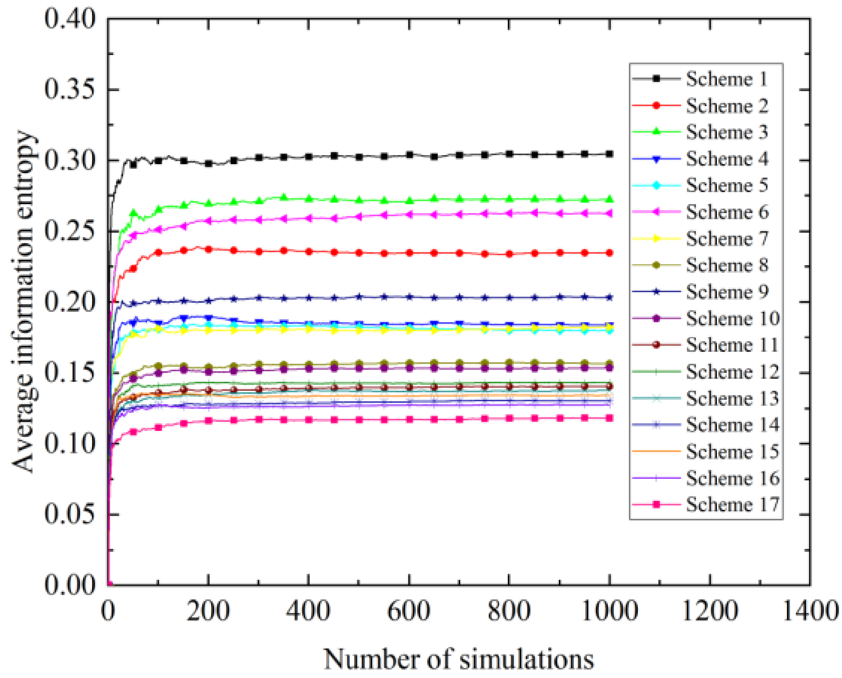

Figure 8. Relationship between average information entropy and number of simulations.

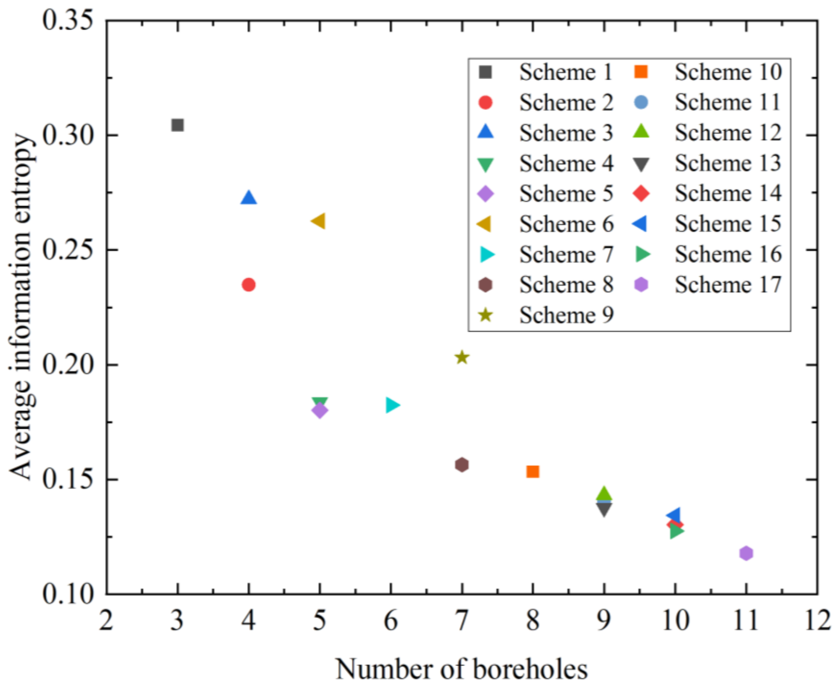

Figure 9. Variations of average information entropy with number of boreholes.

3.3. Stability Analysis of Unsaturated Soil Slope Considering Stratigraphic Uncertainty

3.3.1. FEM Model of Slope

The FEM model of unsaturated soil slope is shown in Figure 10. The slope is affected by gravity, and the gravity acceleration is 10 m/s^2. The left and right sides of the slope are fixed in the horizontal direction. The bottom boundary is fixed in both the horizontal and vertical directions. The matric suction of the area 3 m down from the surface is set to be 60 kPa [28]. The groundwater tables at the left and right sides of the slope are 15 m and 9 m (0 at the bottom), respectively, and other boundaries of the slope are impermeable.

Three virtual groundwater table observation boreholes (BW1, BW2 and BW3) are arranged at the top, middle and toe of the slope to observe the groundwater table in the vicinity of the slope. The parameters of the unsaturated soil are shown in Table 2. Here, the van Genuchten model with two parameters, a and n, are used for describing the SWCC curve of unsaturated soil. The SWCC curves of the three types of soil are shown in Figure 11.

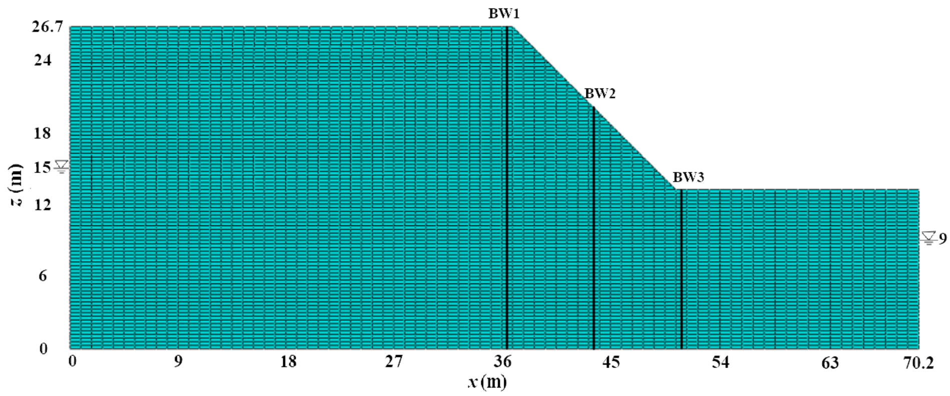

Figure 10. FEM model of slope.

Table 2. Parameters of the three types of soils.

Soil Type	Unit Weight, γ (kN/m^3)	Elastic Modulus, E (MPa)	Poisson's Ratio, ν	Effective Cohesion, c (kPa)	Effective Friction Angle, φ (Degree)	Fully Saturated Hydraulic Conductivity, k (m/s)	a (kPa)	n
Clay	20	30	0.3	18	25	5×10^{-5}	100	1.5
Sand	20	50	0.3	2	33	5×10^{-4}	10	2.5
Silt	20	30	0.3	6	28	1×10^{-4}	20	2.0

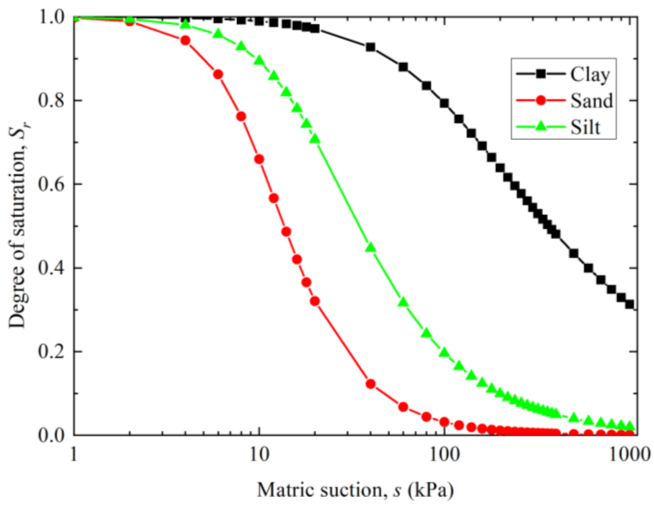

Figure 11. SWCC curves of the three types of soil.

3.3.2. Stability of Unsaturated Soil Slope for Different Borehole Schemes

The slope stability is analyzed under the "real" stratum at first using ABAQUS software based on the strength reduction method. To consider the groundwater table in the vicinity of the slope, as shown in Figure 10, three groundwater tables at the top, middle and toe of the slope, are extracted from the odb files and the average value of the three groundwater tables is denoted as AGT in this paper. For the slope with the "real" stratum, the "real" values of FS and AGT are 1.213 and 13.507 m, respectively. As discussed in

Section 3.2.3, the degree of stratum uncertainty is different among the 17 borehole schemes. Since the stability of unsaturated soil slope is closely related to the strata, the statistics of FS will also be different among the borehole schemes. In this section, the developed stability analysis algorithm for unsaturated soil slope considering stratigraphic uncertainty is used to calculate the FS and the AGT under various borehole schemes, and the results are analyzed.

The number of Monte Carlo simulations has a significant impact on the statistics of FS and AGT. In this paper, different numbers of simulations are taken for Scheme 7 (randomly selected), and the variations of statistics of FS and AGT with a number of simulations are drawn in Figures 12 and 13, respectively. According to Figures 12 and 13, when the number of simulations is greater than 400, the mean value and standard deviation of FS and AGT are all stable. Therefore, the number of Monte Carlo simulations is taken as 400.

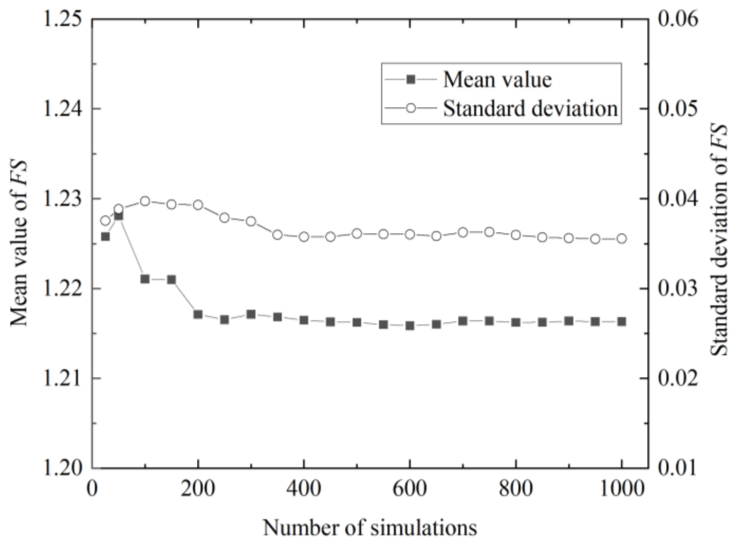

Figure 12. Variations of mean value and standard deviation of FS with number of simulations.

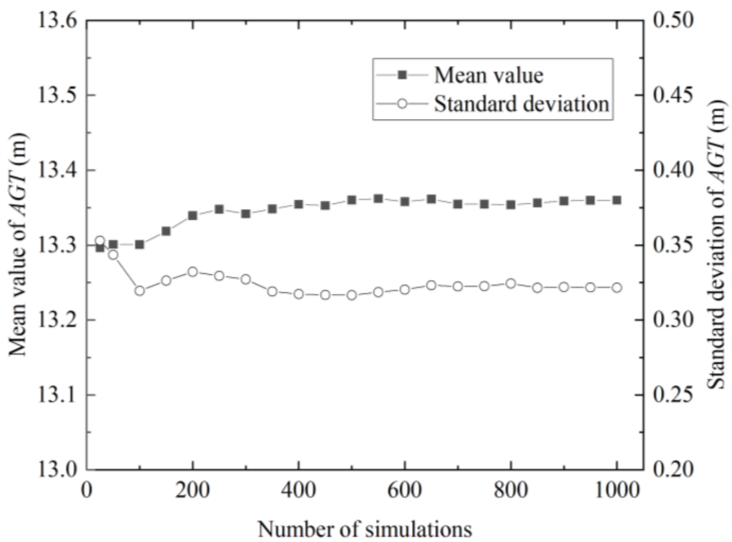

Figure 13. Variations of mean value and standard deviation of AGT with number of simulations.

The statistics of FS and AGT for different boreholes are shown in Figure 14. It can be seen that the number of boreholes and the location of boreholes have an important impact on the statistics of FS and AGT. For example, when the number of boreholes is set to be five, there are three schemes, namely Scheme 4, Scheme 5 and Scheme 6. The statistics of FS and AGT show significant differences among these three schemes, indicating that the location of boreholes exerts on the stability of the slope and the groundwater table. When the number of boreholes is different, the statistics of FS and AGT are also significantly different. With the increase in the number of boreholes, the mean values of FS and AGT do not increase or decrease monotonically. This is because the additional borehole information may make the predicted stratum closer to or deviate from the "real" stratum. To further study the influence of borehole number, the trend lines of the statistics of FS and AGT are drawn in Figure 14. It can be seen from the trend lines that the mean values of FS and AGT gradually approach and finally converge to the real values with the increase in the borehole number. It is because as the number of boreholes increases, "bad" data exists, while "good" data dominates. The standard deviations of FS and AGT basically decrease with the increase in the borehole number. It implies that a greater number of known boreholes in the scheme leads to a greater probability that the mean values of FS and AGT are closer to the real values and a greater probability that the standard deviations of FS and AGT are less. In practical engineering, some additional boreholes may lead to a deviation between the calculated mean value of FS (or AGT) and the real value, as the added boreholes may be "bad" data. However, the number of boreholes should be obtained as much as possible. Because the overall trend is that the more boreholes are drilled, the closer the calculated mean value of FS (or AGT) is to the real value, and the more stable the estimation of FS (or AGT). On the other hand, if the stratagraphic uncertainty is ignored, the calculated FS (or AGT) is more likely to be close to the real value. The standard deviations of both FS and AGT are related to the uncertainty of strata, and the relationship between the standard deviation of FS and the standard deviation of AGT is drawn in Figure 15. It is found that the Pearson's R between them is 0.986, indicating that there is a good linear relationship between them. The standard deviation of FS increases with the increase in the standard deviation of AGT.

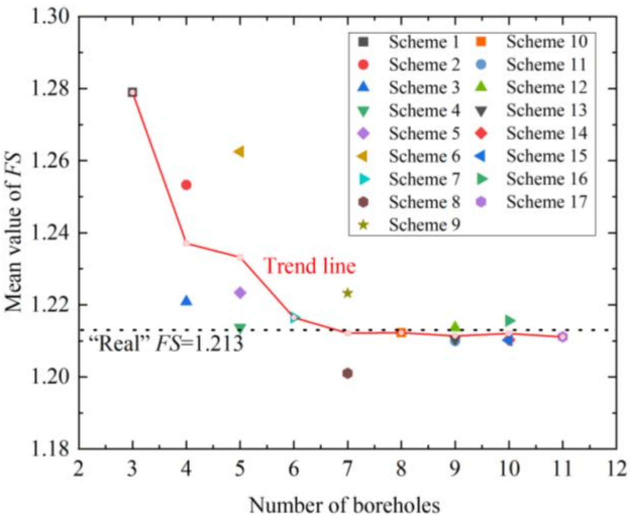

(**a**) Mean value of FS

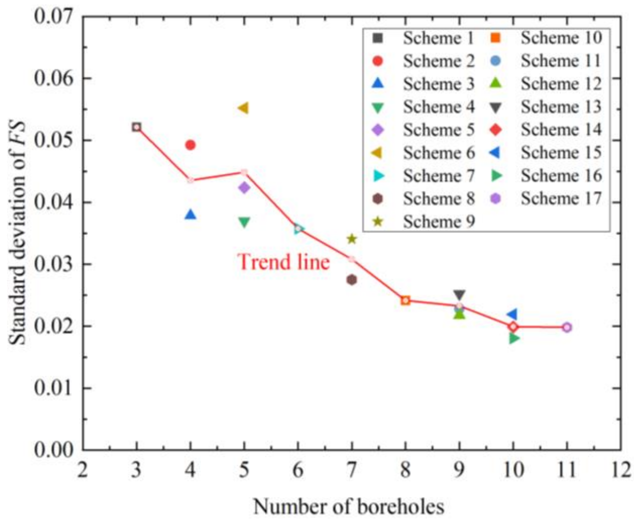

(**b**) Standard deviation of FS

Figure 14. *Cont.*

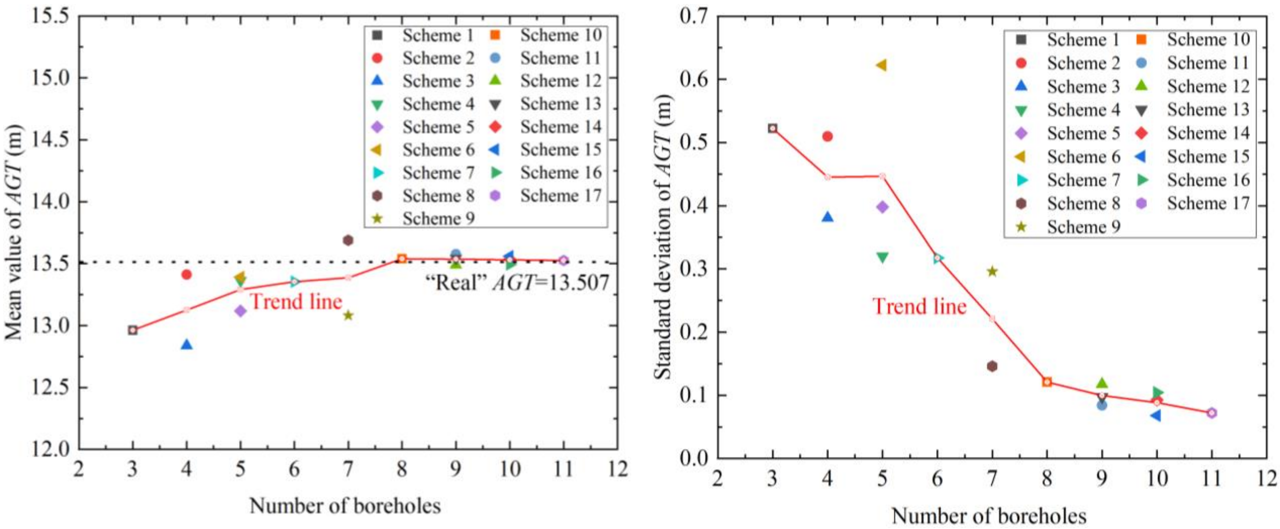

(**c**) Mean value of AGT (**d**) Standard deviation of AGT

Figure 14. Statistics of FS and AGT for different borehole schemes.

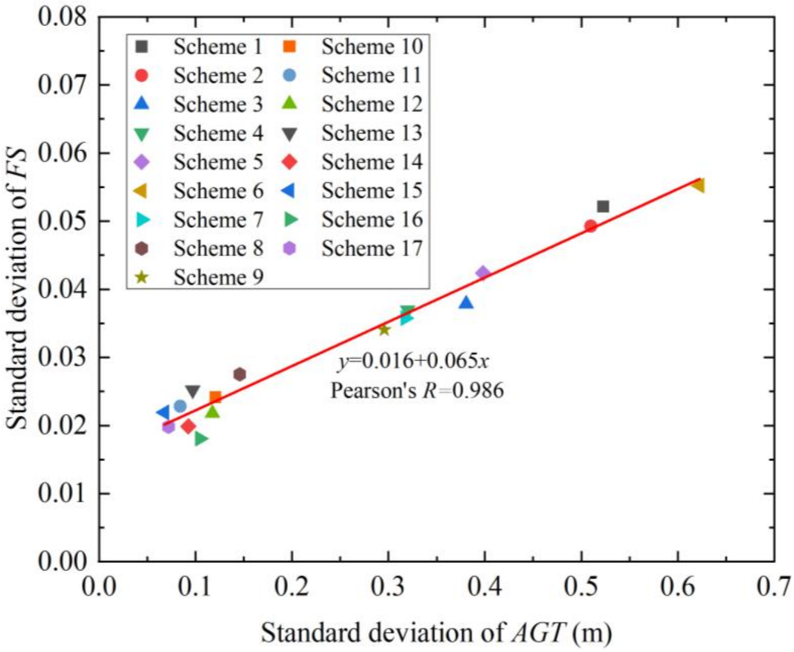

Figure 15. Relationship between the standard deviation of FS and the standard deviation of AGT.

3.3.3. Relationship between the Standard Deviation of FS (or AGT) and the Average Information Entropy

As mentioned in Section 3.3.2, the standard deviation of FS (or AGT) is related to the uncertainty of the strata. The level of stratigraphic uncertainty can be quantified using the average information entropy AVH; therefore, the relationship between the standard deviation of FS (or AGT) and the AVH is drawn in Figure 16 (or Figure 17). It can be seen from Figure 16 that the Pearson's R between the standard deviation of the FS and the AVH is 0.901, which shows that there is a good linear relationship between them. The greater the AVH, the stronger the uncertainty of the stratum and the greater the standard deviation of FS. Similarly, there also exists a good linear relationship between the standard deviation of AGT and the AVH, and the Pearson's R between them is 0.909 (see Figure 17).

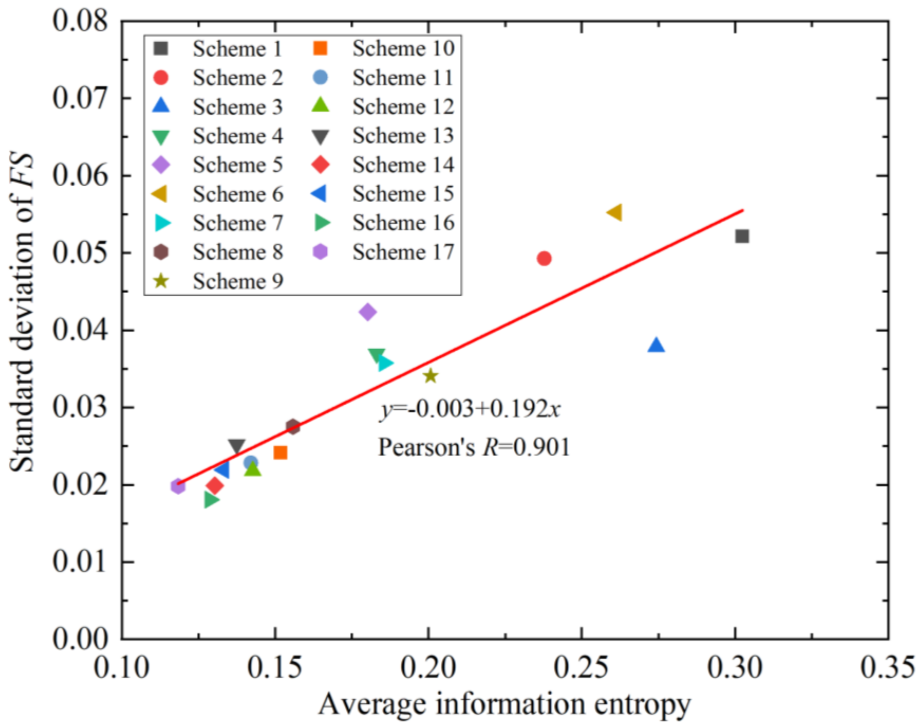

Figure 16. Relationship between the standard deviation of *FS* and the *AVH*.

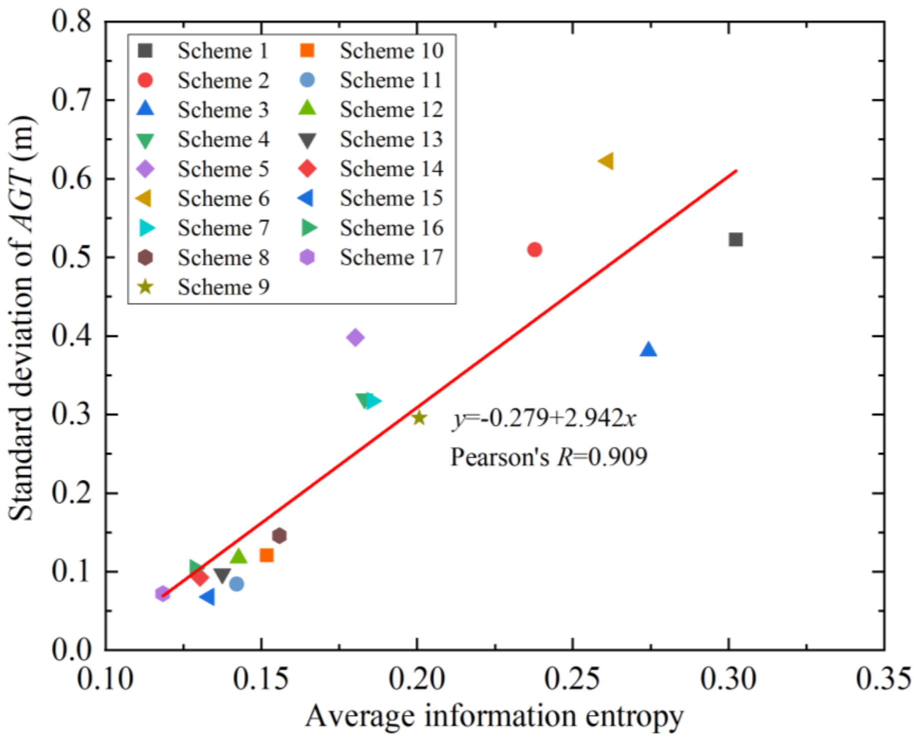

Figure 17. Relationship between the standard deviation of *AGT* and the *AVH*.

3.3.4. Relationship between *FS* and *AGT* for Different Schemes

The groundwater table significantly influences the safety factor of the unsaturated soil slope for the case with a deterministic stratum. Here, the relationship between *FS* and *AGT* is investigated considering the uncertainty of strata. It is noted that the groundwater tables at the left and right boundaries of the stratum are deterministic in this case, so the variation of the groundwater table in the stratum is completely caused by the uncertainty of the stratum. The relationship between FS and AGT for different schemes is shown in Figure 18. It can be seen from Figure 18 that the distribution of sample points of various borehole schemes is different. Most of the sample points are centralized and distributed in a downward-inclined band, and some scattered sample points are distributed below the band. Especially for the boreholes schemes with more than six boreholes (Schemes 8, 10, 11, 14 and 17), the scattered sample points are more obvious. This phenomenon may be attributed to the fact that FS is more sensitive to the local soil type distribution, whereas AGT is not. The widths of the bands are different among the borehole schemes, and they are related to the uncertainty of the stratum. When there are fewer known boreholes, the uncertainty of the stratum is generally greater, and the band is wider. The sample points are linearly fitted, and the parameters of linear fitting are listed in Table 3. When the borehole number is less than or equal to 6 (Schemes 1, 2, 4 and 7), the absolute values of Pearson's R vary from 0.596 to 0.717, indicating that there is a strong linear relationship between FS and AGT. When the borehole number is larger than six (Schemes 8, 10, 11, 14 and 17), the absolute values of Pearson's R vary from 0.161 to 0.410, indicating that there is a weak linear relationship between FS and AGT. The slope of the fitting line B varies among the borehole schemes, ranging from −0.044 to −0.077. The values of B are negative for all the borehole schemes, which means that FS is negatively related to AGT. The greater the absolute value of B, the more sensitive FS is to AGT.

Table 3. Parameters of linear fitting for the sample points of different borehole schemes.

Borehole Schemes	Borehole Number	Intercept A	Slope B	Pearson's R	Residual Sum of Squares
1	3	2.050	−0.059	−0.596	0.700
2	4	2.182	−0.069	−0.717	0.471
4	5	2.146	−0.070	−0.604	0.346
7	6	2.223	−0.075	−0.669	0.282
8	7	2.256	−0.077	−0.410	0.251
10	8	2.162	−0.070	−0.351	0.204
11	9	1.801	−0.044	−0.161	0.202
14	10	1.835	−0.046	−0.217	0.150
17	11	2.068	−0.063	−0.231	0.148

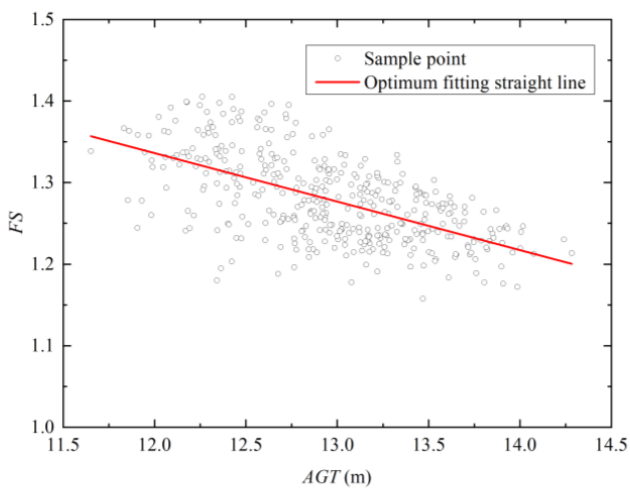

(**a**) Scheme 1

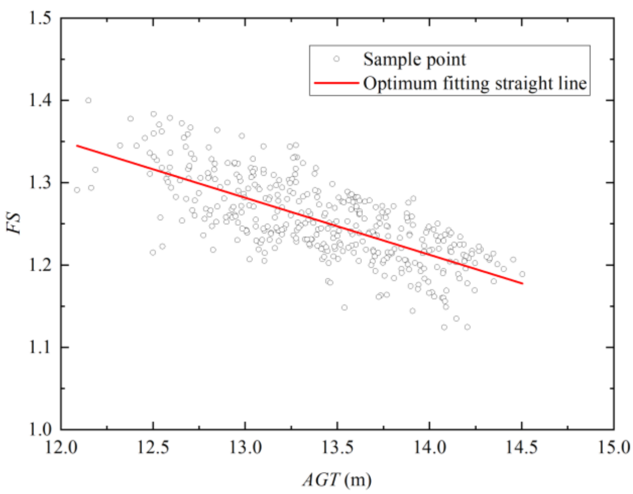

(**b**) Scheme 2

Figure 18. *Cont.*

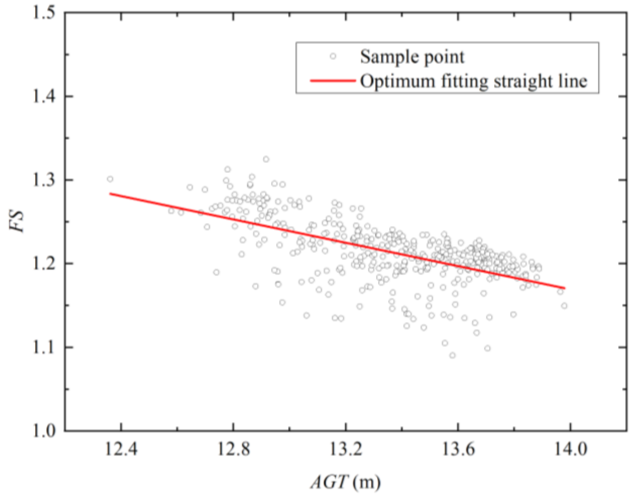

(**c**) Scheme 4

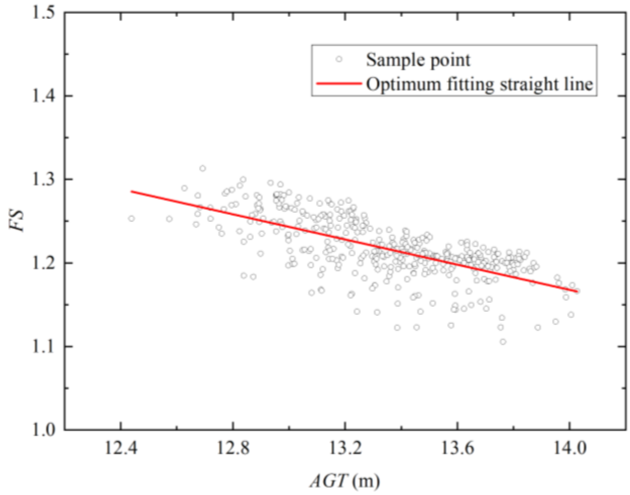

(**d**) Scheme 7

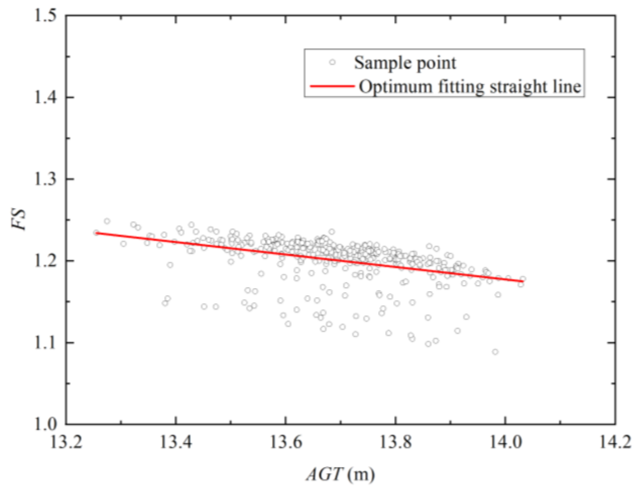

(**e**) Scheme 8

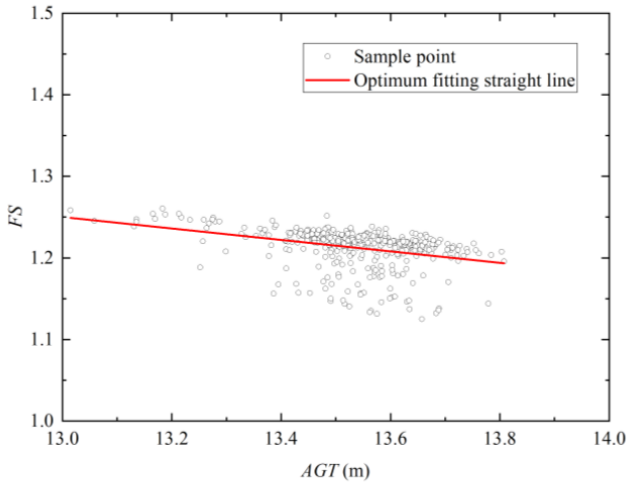

(**f**) Scheme 10

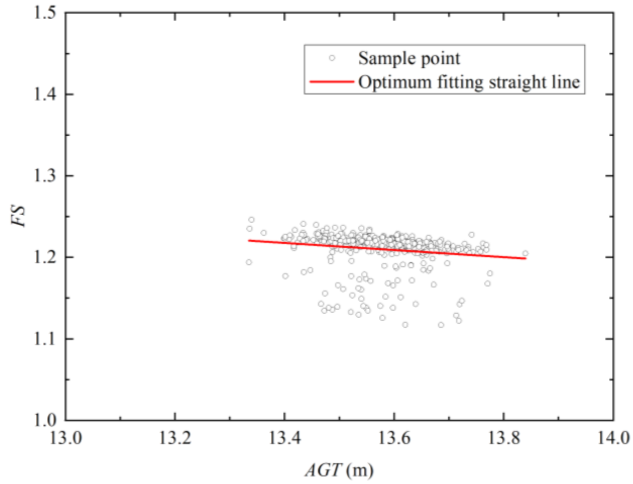

(**g**) Scheme 11

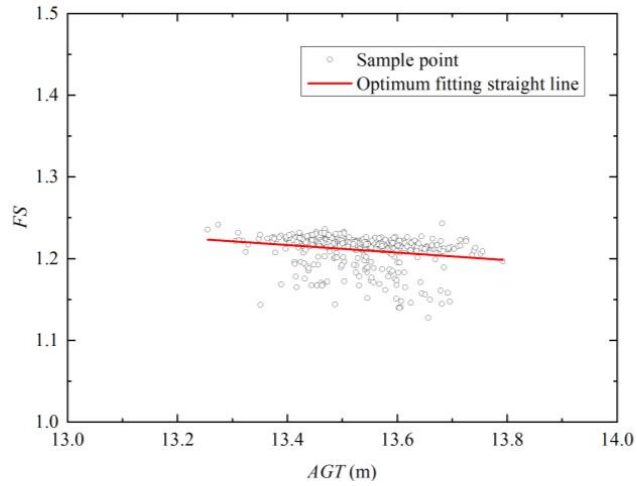

(**h**) Scheme 14

Figure 18. *Cont.*

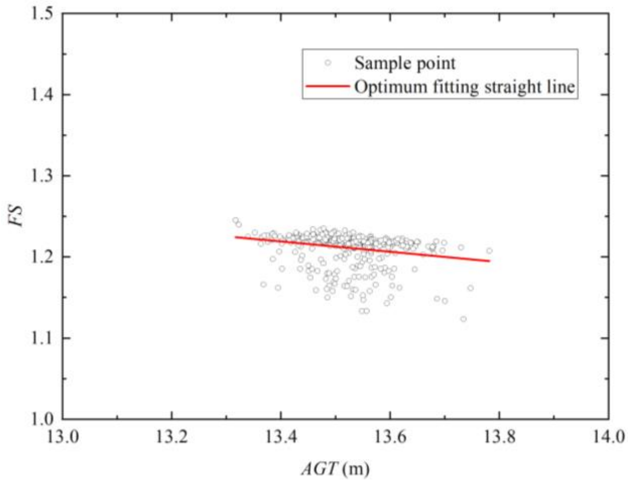

(**i**) Scheme 17

Figure 18. Relationship between *FS* and *AGT* for various borehole schemes.

4. Conclusions

In this paper, stratigraphic uncertainty is simulated using the enhanced CMC model which has the advantage of high accuracy in simulating strata [24] and stratigraphic uncertainty is quantified by information entropy. The effect of borehole schemes on the level of stratigraphic uncertainty and the stability of unsaturated soil slope is evaluated through a typical stratum in Australia using the proposed algorithm. The following conclusions can be drawn from the study:

(1) Information entropy can well quantify the overall and local uncertainty of strata. There is a linear relationship between the standard deviation of the *FS* (or *AGT*) and the average information entropy. Since the calculation of information entropy is simple and fast, the variation of *FS* and *AGT* can be estimated by information entropy in practical engineering.

(2) When the number of boreholes is 11, the mean values of *FS* and *AGT* are close to the "real" values, which proves that the proposed algorithm can accurately calculate the *FS* and *AGT*. The statistics of *FS* and *AGT* will not monotonically increase or decrease with the increase in the borehole number. But the trend is that the mean values of *FS* and *AGT* gradually approach and eventually converge to the real values and the standard deviations of *FS* and *AGT* decrease. Therefore, when there are more known boreholes, the mean value of *FS* (or *AGT*) is more likely to be close to the real value, and the standard deviation of *FS* (or *AGT*) is more likely to be small. Although some additional boreholes may be "bad" data and increase the deviation between the estimated values of *FS* and *AGT* and the true values, the overall trend is still that the more boreholes are drilled, the more accurate the estimation is. Increasing boreholes is beneficial in practical engineering.

(3) The sample points with *AGT* and *FS* as abscissa and ordinate, respectively, are centralized and distributed in a downward inclined band, and some scattered sample points are distributed below the band, especially for the borehole schemes with more than six boreholes. The widths of the bands are related to the uncertainty of the stratum. The *FS* and the *AGT* are negatively correlated considering stratigraphic uncertainty. In practical engineering, the *FS* of slope can be roughly estimated by observing the groundwater table according to this negative correlation property. However, the estimated results are not deterministic, have probabilistic properties and have a certain level of credibility.

(4) The influence of stratigraphic uncertainty on the stability of unsaturated soil slopes is investigated in this paper. In the future, we will consider both the stratigraphic

uncertainty and uncertainty of soil parameters and study their influence on the stability of unsaturated soil slopes.

Author Contributions: Conceptualization, W.C.; Data curation, W.C. and Z.W.; Funding acquisition, W.C.; Methodology, W.C. and W.L.; Software, W.C.; Validation, W.C. and W.L.; Visualization, W.L.; Writing—original draft, W.C. and Z.W.; Writing—review and editing, W.C. All authors have read and agreed to the published version of the manuscript.

Funding: This research was funded by National Natural Science Foundation of China (Project Nos. 42177170, 52004090), Natural Science Foundation of Hebei Province (No. E2021508031), Langfang Science and Technology Research and Development Program (No. 2020013026) and Fundamental Research Funds for the Central Universities (No. 3142021010).

Institutional Review Board Statement: Not applicable.

Informed Consent Statement: Not applicable.

Data Availability Statement: Not applicable.

Conflicts of Interest: The authors declare no conflict of interest.

References

1. Phoon, K.K.; Kulhawy, F.H. Characterization of geotechnical variability. *Can. Geotech. J.* **1999**, *36*, 612–624. [CrossRef]
2. Elkateb, T.; Chalaturnyk, R.; Robertson, P.K. An overview of soil heterogeneity: Quantification and implications on geotechnical field problems. *Can. Geotech. J.* **2003**, *40*, 1–15. [CrossRef]
3. Deng, Z.P.; Li, D.Q.; Qi, X.H.; Cao, Z.J.; Phoon, K.K. Reliability evaluation of slope considering stratigraphic uncertainty and inherent variability of soil parameters. *Comput. Geotech.* **2017**, *92*, 121–131. [CrossRef]
4. Gong, W.; Zhao, C.; Juang, C.H.; Zhang, Y.; Tang, H.; Lu, Y. Coupled characterization of stratigraphic and geo-properties uncertainties–a conditional random field approach. *Eng. Geol.* **2021**, *294*, 106348. [CrossRef]
5. Griffiths, D.V.; Fenton, G.A. Probabilistic slope stability analysis by finite elements. *J. Geotech. Geoenviron. Eng.* **2004**, *130*, 507–518. [CrossRef]
6. Jiang, S.H.; Huang, J. Modeling of non-stationary random field of undrained shear strength of soil for slope reliability analysis. *Soils Found* **2018**, *58*, 185–198. [CrossRef]
7. Zhu, H.; Zhang, L.M. Characterizing geotechnical anisotropic spatial variations using random field theory. *Can. Geotech. J.* **2013**, *50*, 723–734. [CrossRef]
8. Johari, A.; Fooladi, H. Comparative study of stochastic slope stability analysis based on conditional and unconditional random field. *Comput. Geotech.* **2020**, *125*, 103707. [CrossRef]
9. Tang, W.H.; Sidi, I.; Gilbert, R.B. Average property in random two-state medium. *J. Eng. Mech.* **1989**, *115*, 131–144. [CrossRef]
10. Kohno, S.; Ang, H.S.; Tang, W.H. Reliability evaluation of idealized tunnel systems. *Struct. Saf.* **1992**, *11*, 81–93. [CrossRef]
11. Elfeki, A.; Dekking, M. A Markov chain model for subsurface characterization: Theory and applications. *Math. Geol.* **2001**, *33*, 569–589. [CrossRef]
12. Elfeki, A.; Dekking, F.M. Modelling subsurface heterogeneity by coupled Markov chains: Directional dependency, Walther's law and entropy. *Geotech. Geol. Eng.* **2005**, *23*, 721–756. [CrossRef]
13. Li, Z.; Wang, X.; Wang, H.; Liang, R.Y. Quantifying stratigraphic uncertainties by stochastic simulation techniques based on markov random field. *Eng. Geol.* **2016**, *201*, 106–122. [CrossRef]
14. Wang, X. Uncertainty quantification and reduction in the characterization of subsurface stratigraphy using limited geotechnical investigation data. *Under. Space* **2020**, *5*, 125–143. [CrossRef]
15. Wang, X.; Wang, H.; Liang, R.Y.; Zhu, H.; Di, H. A hidden markov random field model based approach for probabilistic site characterization using multiple cone penetration test data. *Struct. Saf.* **2018**, *70*, 128–138. [CrossRef]
16. Wang, Y.; Huang, K.; Cao, Z. Probabilistic identification of underground soil stratification using cone penetration tests. *Can. Geotech. J.* **2013**, *50*, 766–776. [CrossRef]
17. Cao, Z.J.; Zheng, S.; Li, D.Q.; Phoon, K.K. Bayesian identification of soil stratigraphy based on soil behaviour type index. *Can. Geotech. J.* **2019**, *56*, 570–586. [CrossRef]
18. Alshboul, O.; Shehadeh, A.; Almasabha, G.; Almuflih, A.S. Extreme gradient boosting-based machine learning approach for green building cost prediction. *Sustainability* **2022**, *14*, 6651. [CrossRef]
19. Alshboul, O.; Almasabha, G.; Shehadeh, A.; Mamlook, R.E.A.; Almuflih, A.S.; Almakayeel, N. Machine learning-based model for predicting the shear strength of slender reinforced concrete beams without stirrups. *Buildings* **2022**, *12*, 1166. [CrossRef]
20. Gong, W.; Zhao, C.; Juang, C.H.; Tang, H.; Hu, X. Stratigraphic uncertainty modelling with random field approach. *Comput. Geotech.* **2020**, *125*, 103681. [CrossRef]
21. Shi, C.; Wang, Y. Non-parametric and data-driven interpolation of subsurface soil stratigraphy from limited data using multiple point statistics. *Can. Geotech. J.* **2021**, *58*, 261–280. [CrossRef]

22. Qi, X.H.; Li, D.Q.; Phoon, K.K.; Cao, Z.J.; Tang, X.S. Simulation of geologic uncertainty using coupled Markov chain. *Eng. Geol.* **2016**, *207*, 129–140. [CrossRef]
23. Deng, Z.P.; Jiang, S.H.; Niu, J.T.; Pan, M.; Liu, L.L. Stratigraphic uncertainty characterization using generalized coupled Markov chain. *B. Eng. Geol. Environ.* **2020**, *79*, 5061–5078. [CrossRef]
24. Cao, W.; Zhou, A.; Shen, S.L. An analytical method for estimating horizontal transition probability matrix of coupled Markov chain for simulating stratigraphic uncertainty. *Comput. Geotech.* **2021**, *129*, 103871. [CrossRef]
25. Zhang, J.Z.; Liu, Z.Q.; Zhang, D.M.; Huang, H.W.; Phoon, K.K.; Xue, Y.D. Improved coupled Markov chain method for simulating geological uncertainty. *Eng. Geol.* **2022**, *298*, 106539.
26. Qi, X.H.; Li, D.Q.; Zhou, C.; Phoon, K.K. Estimation of horizontal transition probability matrix for coupled Markov chain based on borehole data. *J. Basic Sci. Eng.* **2017**, *25*, 967–984.
27. Li, J.; Cai, Y.; Li, X.; Zhang, L. Simulating realistic geological stratigraphy using direction-dependent coupled Markov chain model. *Comput. Geotech.* **2019**, *115*, 103147. [CrossRef]
28. Cho, S.E.; Lee, S.R. Instability of unsaturated soil slopes due to infiltration. *Comput. Geotech.* **2001**, *28*, 185–208. [CrossRef]
29. Cho, S.E.; Lee, S.R. Evaluation of surficial stability for homogeneous slopes considering rainfall characteristics. *J. Geotech. Geoenviron. Eng.* **2002**, *128*, 756–763. [CrossRef]
30. Griffiths, D.V.; Lu, N. Unsaturated slope stability analysis with steady infiltration or evaporation using elasto-plastic finite elements. *Int. J. Numer. Anal. Met.* **2005**, *29*, 249–267. [CrossRef]
31. Ray, R.L.; Jacobs, J.M.; Alba, P.D. Impacts of unsaturated zone soil moisture and groundwater table on slope instability. *J. Geotech. Geoenviron. Eng.* **2010**, *136*, 1448–1458. [CrossRef]
32. Li, W.C.; Lee, L.M.; Cai, H.; Li, H.J.; Dai, F.C.; Wang, M.L. Combined roles of saturated permeability and rainfall characteristics on surficial failure of homogeneous soil slope. *Eng. Geol.* **2013**, *153*, 105–113. [CrossRef]
33. Cuomo, S.; Di Perna, A.; Martinelli, M. Modelling the spatio-temporal evolution of a rainfall-induced retrogressive landslide in an unsaturated slope. *Eng. Geol.* **2021**, *294*, 106371. [CrossRef]
34. Yan, T.; Xiong, J.; Ye, L.; Gao, J.; Xu, H. Field investigation and finite element analysis of landslide-triggering factors of a cut slope composed of granite residual soil: A case study of Chongtou Town, Lishui City, China. *Sustainability* **2023**, *15*, 6999. [CrossRef]
35. Jia, J.; Pei, X.; Liu, G.; Cai, G.; Guo, X.; Hong, B. Failure mechanism of anti-dip layered soft rock slope under rainfall and excavation conditions. *Sustainability* **2023**, *15*, 9398. [CrossRef]
36. Santoso, A.M.; Phoon, K.K.; Quek, S.T. Effects of soil spatial variability on rainfall-induced landslides. *Comput. Geotech.* **2011**, *89*, 893–900. [CrossRef]
37. Ali, A.; Huang, J.; Lyamin, A.V.; Sloan, S.W.; Griffiths, D.V.; Cassidy, M.J.; Li, J.H. Simplified quantitative risk assessment of rainfall-induced landslides modelled by infinite slopes. *Eng. Geol.* **2014**, *179*, 102–116. [CrossRef]
38. Cho, S.E. Probabilistic stability analysis of rainfall-induced landslides considering spatial variability of permeability. *Eng. Geol.* **2014**, *171*, 11–20. [CrossRef]
39. Dou, H.Q.; Han, T.C.; Gong, X.N.; Qiu, Z.Y.; Li, Z.N. Effects of the spatial variability of permeability on rainfall-induced landslides. *Eng. Geol.* **2015**, *192*, 92–100. [CrossRef]
40. Zhou, A.; Li, C.Q.; Huang, J. Failure analysis of an infinite unsaturated soil slope. *Geotech. Eng.* **2016**, *169*, 410–420. [CrossRef]
41. Johari, A.; Gholampour, A. A practical approach for reliability analysis of unsaturated slope by conditional random finite element method. *Comput. Geotech.* **2018**, *102*, 79–91. [CrossRef]
42. Masoudian, M.S.; Afrapoli, M.; Tasalloti, A.; Marshall, A.M. A general framework for coupled hydro-mechanical modelling of rainfall-induced instability in unsaturated slopes with multivariate random fields. *Comput. Geotech.* **2019**, *115*, 103162. [CrossRef]
43. Srivastava, A.; Babu, G.; Haldar, S. Influence of spatial variability of permeability property on steady state seepage flow and slope stability analysis. *Eng. Geol.* **2010**, *110*, 93–101. [CrossRef]
44. Jiang, S.H.; Li, D.Q.; Zhou, C.B.; Zhang, L.M. Reliability analysis of unsaturated slope considering spatial variability. *Rock Soil Mech.* **2014**, *35*, 2569–2578.
45. Le, T.; Gallipoli, D.; Sanchez, M.; Wheeler, S. Stability and failure mass of unsaturated heterogeneous slopes. *Can. Geotech. J.* **2015**, *52*, 1747–1761. [CrossRef]
46. Le, T.; Sanchez, M.; Gallipoli, D.; Wheeler, S. Probabilistic study of rainfall-triggered instabilities in randomly heterogeneous unsaturated finite slopes. *Transport Porous Med.* **2019**, *126*, 199–222. [CrossRef]
47. Ng, C.W.W.; Qu, C.; Ni, J.; Guo, H. Three-dimensional reliability analysis of unsaturated soil slope considering permeability rotated anisotropy random fields. *Comput. Geotech.* **2022**, *151*, 104944.
48. Rotaru, A.; Bejan, F.; Almohamad, D. Sustainable slope stability analysis: A critical study on methods. *Sustainability* **2022**, *14*, 8847. [CrossRef]
49. Li, D.Q.; Qi, X.H.; Cao, Z.J.; Tang, X.S.; Phoon, K.K.; Zhou, C.B. Evaluating slope stability uncertainty using coupled markov chain. *Comput. Geotech.* **2016**, *73*, 72–82. [CrossRef]
50. Liu, L.L.; Cheng, Y.M.; Pan, Q.J.; Dias, D. Incorporating stratigraphic boundary uncertainty into reliability analysis of slopes in spatially variable soils using one-dimensional conditional Markov chain model. *Comput. Geotech.* **2019**, *118*, 103321. [CrossRef]
51. Gong, W.; Tang, H.; Wang, H.; Wang, X.R.; Juang, H. Probabilistic analysis and design of stabilizing piles in slope considering stratigraphic uncertainty. *Eng. Geol.* **2019**, *259*, 105162.

52. Ghadrdan, M.; Dyson, A.P.; Shaghaghi, T.; Tolooiyan, A. Slope stability analysis using deterministic and probabilistic approaches for poorly defined stratigraphies. *Geomech. Geophys. Geo-Energ. Geo-Resour.* **2021**, *7*, 4. [CrossRef]
53. Deng, Z.P.; Pan, M.; Niu, J.T.; Jiang, S.H. Full probability design of soil slopes considering both stratigraphic uncertainty and spatial variability of soil properties. *Bull. Eng. Geol. Environ.* **2022**, *81*, 195. [CrossRef]
54. Zhang, J.Z.; Huang, H.W.; Zhang, D.M.; Phoon, K.K.; Tang, C. Quantitative evaluation of stratigraphic uncertainty and its influence on tunnel structural performance using improved coupled Markov chain. *Acta Geotech.* **2021**, *16*, 3709–3724. [CrossRef]
55. Cao, W.; Zhou, A. An improved coupled Markov chain model for simulating geological uncertainty. In Proceedings of the 8th International Symposium on Geotechnical Safety and Risk (ISGSR), Newcastle, Australia, 14–16 December 2022.